Available online at www.sciencedirect.com
SCIENCE DIRECT®
Polymer 44 (2003) 4557–4562
polymer
www.elsevier.com/locate/polymer

Micromechanical properties of glassy and rubbery polymer brush layers as probed by atomic force microscopy

D. Julthongpiput, M. LeMieux, V.V. Tsukruk*

Department of Materials Science and Engineering, Iowa State University, 3053 Gilman Hall, Ames, IA 50011, USA

Received 17 February 2003; received in revised form 6 May 2003; accepted 8 May 2003

Abstract

Carboxylic acid terminated polystyrene and polybutylacrylate were grafted from melt onto a silicon substrate modified with the epoxysilane monolayer. The tethered layers fabricated from polymers of different molecular weights are smooth, uniform, mechanically stable, and cover homogeneously the modified silicon surface. Micromechanical properties of the dry glassy and rubbery brush layers were measured with atomic force microscope. We observed that for the PS layers with the thickness higher than 7 nm, the average value of the elastic moduli reached 1.1 GPa, which is close, but still lower than the expected for bulk polymer. The elastic modulus of PS polymer brush layers dramatically depends upon molecular weight and follows the inverse law with segment molecular weight, M_c of 18,000 known for bulk PS. This result indicates that the process of the formation of the physical network within polymer melt of chains tethered to a solid substrate is similar to that occurring in unconstrained polymer melt. Under these conditions, three PS brush layers studied in this work represent different cases of chains without stable entanglements for $M < M_c$ as well as chains with stable entanglements for brushes with $M \sim M_c$. This transition shows itself in significant reduction of the compliance reflected in twofold increase in elastic modulus. Our estimation predicts that modest lowering of 'limiting' elastic modulus of 1.4 GPa can be expected for thicker polymer brushes.

Keywords: Grafted polymers; Micromechanical properties; Atomic force microscopy

1. Introduction

A variety of modern applications require robust ultrathin coatings with molecularly controllable surface properties. It is often desirable to modify interfaces uniformly and permanently with selectively adsorbed polymers [1,2,3]. In fact, in experimental studies of friction and boundary lubrication, it has been found that covalently or strongly bound lubricant layers are more effective in protecting sliding surfaces against wear than physisorbed molecular layers that are easily removed or lifted off due to their weak binding to the surface [4,5,6]. Hydrocarbon and fluorocarbon liquid lubricants also reduce friction and offer protection against damage, but these films similarly break down at high loads, again, due to their weak binding to the surfaces. In both cases, the friction ends up being load-controlled, resulting in high friction and wear [7].

Ultrathin, end-grafted polymer brush layers can dramatically affect the surface properties of substrates such as adhesion, lubrication, wettability, friction, and biocompatibility [8,9,10]. Polymer brushes are long chain polymer molecules attached by one end to a surface, with a grafting density high enough so that the chains are obliged to stretch away from the surface. This situation is quite different from the typical behavior of flexible polymer chains in a solution, where the long molecules adopt random-walk configurations. The equilibrium conformation of end-grafted chains arises from a balance between polymer–polymer and polymer–solvent interactions, as for unattached chains. Grafted chains stretch away from the surface in order to reduce their interaction with other chains, attaining a different conformation than the optimal for free chains in bulk or in solution. Different models [11,12,13] for the segment density profile normal to the surface and the interactions between two opposed surfaces have been developed for different solvent conditions and regions of overlap (stretching), based on this balance between osmotic pressure and elastic restoring force. In order of increasing overlap (decreasing distance between attachment points),

* Corresponding author. Tel.: +1-515-294-6904; fax: +1-515-294-5444.
E-mail address: vladimir@iastate.edu (V.V. Tsukruk).

0032-3861/03/$ - see front matter © 2003 Elsevier Science Ltd. All rights reserved.
doi:10.1016/S0032-3861(03)00404-X

the model regions are called pancake, mushroom, and brush layers [14].

The grafted brush layer can be fabricated from either solution or melt [15–17]. It is commonly observed that only layers with low grafting density can be obtained by adsorption of polymer from solution, since after some chains have become attached, incoming chains have to diffuse against a concentration gradient to reach the solid surface. In addition, there is an entropy loss arising from the change in conformation of both the incoming and the adsorbed polymer to accommodate another chain. For these reasons, typically only a few milligrams of polymer per square meter adsorb onto a solid surface from a good or θ solvent, regardless of whether the chains become chemically or physically bound to the surface [18].

The irreversible grafting from the melt offers potential advantages over the grafting from solution mainly due to the screening of the excluded volume interactions [19] Presumably, more densely grafted layers can be formed from the melt than from solution. However, until now, there has been no clear understanding on if properties of molecularly thick brush layers from different polymers of different molecular weights fabricated from the melt by the 'grafting to' technique are comparable to ones known for analogous bulk polymers. Moreover, study of their surface properties, such as mechanical, represents a significant challenge for conventional experimental techniques.

The aim of the present study is (i) to fabricate the permanent grafting of a dense and homogeneous polymer layer from melt onto a modified silicon surface and (ii) to study their nanomechnical and surface properties by using atomic force microscopy (AFM). In this study, we have chosen two representative polymers, carboxylic acid terminated polystyrene and polybutylacrylate, representing glassy and rubbery polymers with very different surface properties. The polymer brushes were formed by a grafting from melt technique according to the usual approach established in our lab and described in detail earlier [20]. The epoxysilane self-assembled monolayer (SAM) deposited on a silicon wafer was used as an anchoring surface. We previously showed that the epoxy–SAM is homogeneous with terminal epoxy groups mainly located at the SAM surface [16,17].

2. Experimental

Narrow fractions of carboxy-terminated polystyrene (M_w = from 4,500 to 28,500, $M_w/M_n = 1.08$) and poly-*t*-butylacrylate ($M_w = 6,500$; $M_w/M_n = 1.06$) were obtained from Polymer Source, Inc. For grafted polymer (Fig. 1), the polymer was spin-coated from a 1.5 wt% toluene solution onto the wafers modified with the epoxysilane SAM [21,22]. The thickness of the polystyrene film measured by ellipsometry was about 40 ± 3 nm. The coated wafers were annealed for 15 min to 18 h in a vacuum oven at 150 °C to

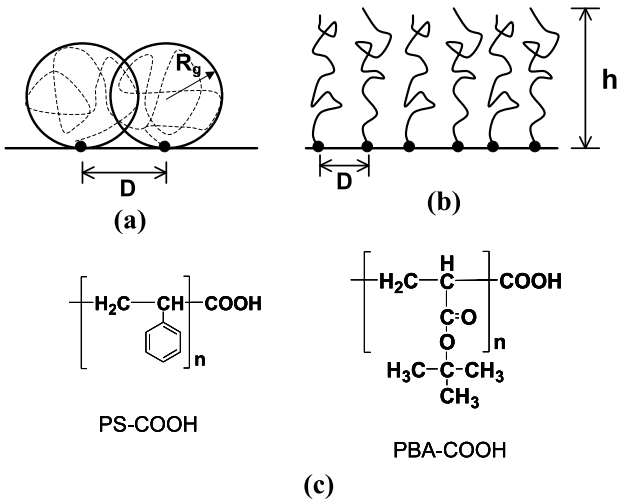

Fig. 1. (a) Schematic representation of neighboring grafted chains in random coil (a) and brush (b) conformations. (c) chemical formulas of the polymers studied: PS–COOH and PBA–COOH.

enable the end groups to graft to the substrate. The ungrafted polymer was removed by multiple washings with toluene and additional washing in an ultrasonic bath.

Ellipsometry was performed using a COMPEL Automatic Ellipsometer (InOmTech, Inc.) with an angle of incidence of 70°. The principles of ellipsometry as well as the experimental details are described elsewhere [23]. The thickness of silicon oxide and epoxysilane SAMs layers were measured independently before grafting polymer layers and were determined to be 1.2 ± 0.1 and 0.7 ± 0.1, respectively. The index of refraction of the silicon oxide, epoxysilane monolayer, polystyrene and polybutylacrylate were considered to be constant and equal to the 'bulk' values 1.46 [24,25], 1.429 [26], 1.59, and 1.464, respectively [27]. All reported thickness values were averaged over six measurements from different locations on the substrate.

AFM-based topographical and micromechanical analysis studies were performed on a Dimension 3000 microscope (Digital Instruments, Inc.) according to the procedure described earlier [28,29]. We used tapping and phase modes to study morphology of these films in ambient air. Silicon tips with spring constants 50 N/m were used. Imaging was done at scan rates in the range 1–2 Hz. For thickness evaluation from AFM data, we used a 'scratch' test. This approach is used frequently for AFM-based measurement of organic and polymer layers and produces reasonable results [30,31].

Contact and friction mode were used to study micromechanical properties of the grafted polymer brush layer. Force–distance data were collected with silicon nitride cantilevers with spring constants in the range of 2–10 N/m as measured by added-mass and resonant frequency techniques [32,33]. Approaching–retracting frequency was in the range of 1–2 Hz and the tip velocity varied from 20 to 100 nm/s. Tip radii (from 10 to 80 nm) were measured by using reference sample with gold nanoparticles

of 5 and 30 nm in diameter and deconvolution procedure [34–36]. To satisfy conditions for elastic mechanical contact, for nanomechanical measurements we selected blunt tips with radius in the range of 50–80 nm.

To obtain surface distribution of surface nanomechanical behavior, we performed force–volume measurements and collected 16 × 16 force–distance curves for the several randomly selected surface areas of 2 μm × 2 μm. From the array of force–distance data, we selected several force–distance curves with the most probable 'apparent' elastic modulus as determined from surface histograms. For selected force–distance curves, we conducted further analysis using the 'double layer' model as an option of a more complicated gradient model [37,38]. This model considers cooperative deformation of two layers with different elastic moduli taking into account the presence of the solid substrate. The reliable values of the elastic modulus can be estimated this way. We adapted the theory to analyze a compliant polymer layer on top of a stiff solid substrate and provided adequate AFM data processing and fitting procedures. Detailed description of our approach is published elsewhere [39].

To characterize the grafted polymer layer, several parameters have been evaluated in accordance with general approaches [4,40]. The amount of grafted polymer, Γ (mg/m^2), was calculated from the ellipsometry and AFM thickness of the layer, h (nm), by the following equation:

$$\Gamma = h\rho \tag{1}$$

where ρ is the density of polymers.

The grafting density, Σ (chain/nm^2), i.e. the inverse of the average area per adsorbed chain, was determined by:

$$\Sigma = \Gamma N_A \times 10^{-21}/M_n = (6.023\Gamma \times 100)/M_n \tag{2}$$

where N_A is Avogadro's number and M_n (g/mol) is the number-average molecular weight of the grafted polymer.

The distance between grafting sites, D (nm), was calculated using the following equation:

$$D = (4/\pi\Sigma)^{1/2} \tag{3}$$

The mean square end-to-end distance (h_Θ, nm) of a non-disturbed polymer chain in bulk state was calculated from

$$h_\Theta = kM_n^{0.5} \tag{4}$$

where k is 0.068 for PBA and the radius of gyration, R_g, was calculated from $R_g = h_\Theta/\sqrt{6}$.

3. Results and discussion

3.1. The kinetics of the formation and morphology of polymer brush layer

The kinetics of the formation and morphology of the grafted PS–COOH layers with different molecular weight of polymers were described in detail elsewhere [41]. Fig. 2 shows the kinetics of formation of the grafted PBA–COOH layers. For this particular polymer, 3 h of the grafting time is enough to approach a virtually constant thickness of the grafted layer. Only statistically insignificant differences were observed for samples with grafting times between 3 and 18 h. The layer heights, h, obtained independently by ellipsometry and AFM measurements, are close to each other (within 5–10% error range). This indicates that the polymer is densely packed in the film with a refractive index (and density) being close to the known value for bulk material.

Fig. 3 and Table 1 show the amount of grafted polymer, grafting density and the surface roughness versus the grafting time of PBA chains. The amount of grafted polymer and grafting density were calculated from Eqs. (1) and (2) (Table 1). Increase of grafting time resulted in a gradual increase of the amount of grafted polymer within first 4 h of grafting. After 18 h of the deposition, the grafted layers practically reach a constant thickness. The amount of grafted polymer reached 3.5 mg/m^2 that is typical for the 'grafted to' technique (1–10 mg/m^2) [42]. Accordingly, grafting density gradually increase to 0.32 chains/nm^2 that is higher than typical grafting densities achievable with grafting to from solution.

Fig. 4 presents AFM topographical images of the grafted PBA polymer layers at different grafting density. Comparison of the images revealed that the films obtained from different grafting densities have different surface morphologies. At low grafting density ($\Sigma \sim 0.1$ chain/nm^2), a surface covered with densely packed islands, a characteristic of dimpled lateral structured predicted and observed for low grafting densities in air as illustrated in Fig. 4(a) [43,44]. This type of morphology was related to the formation of isolated 'mushroom' of grafted polymers in a poor solvent [45]. At intermediate grafting densities (Fig. 4(b) and (c)), the formation of clusters with diameter of 40–50 nm and about 2–3 nm high is observed. A higher grafting density ($\Sigma > 0.3$ chain/nm^2) resulted in a higher level of overlapping of macromolecular chains and the

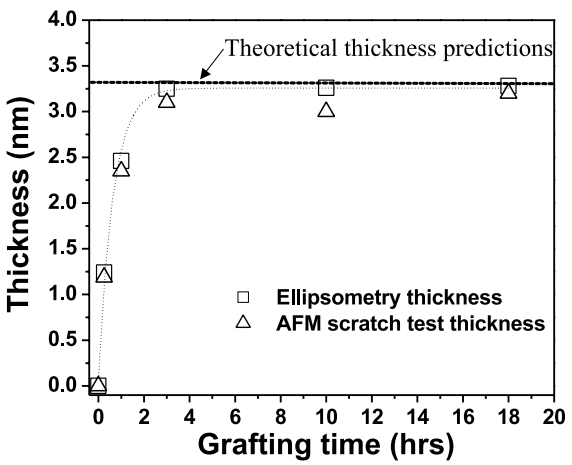

Fig. 2. Thickness of PBA brush layer versus time of the grafting as measured by ellipsometry and AFM.

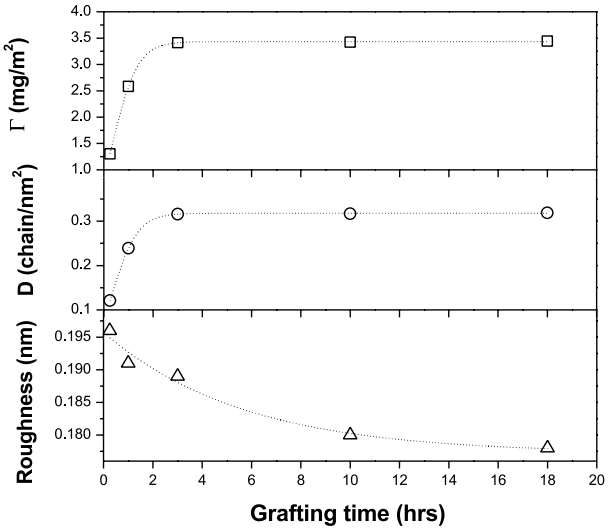

Fig. 3. Grafting amount, grafting density, and microroughness of PBA brush layer versus time of the grafting.

formation of a truly uniform surface morphology as expected for high grafting densities (Fig. 4(d)). A lower value of surface roughness, below 0.17 nm, is observed for these grafted layers (Fig. 3).

The thickness of the dry PBA layer at maximum grafting density reaches 3.0 ± 0.2 nm. This thickness corresponds well to the theoretical estimation, $h = 3.2$ nm, for the polymer brush layer in a poor solvent as estimated from $h \approx N\sigma = N(a/D)^2$ taking $a \approx 0.6$ typical for flexible polymer chains [46,47]. N, σ, and D are the degree of polymerization, dimensionless grafting density, and the distance between grafting sites, respectively. On the other hand, the PBA thickness in a good solvent (toluene) as measured by the AFM is much higher and reaches 9.5 ± 0.5 nm that is consistent with expected thickness of polymer brush in a good solvent [48–51].

3.2. Nanomechanical properties of polymer brush layer

The surface distribution of the mechanical response for the brush layers was obtained with pixel-by-pixel micro-mapping of randomly selected surface areas. An example of histograms of surface distribution of elastic modulus within the 2 μm × 2 μm area for both PS and PBA brush layers is presented in Fig. 5. The average value of the elastic modulus is about 1.1 GPa for the PS layer with the highest molecular

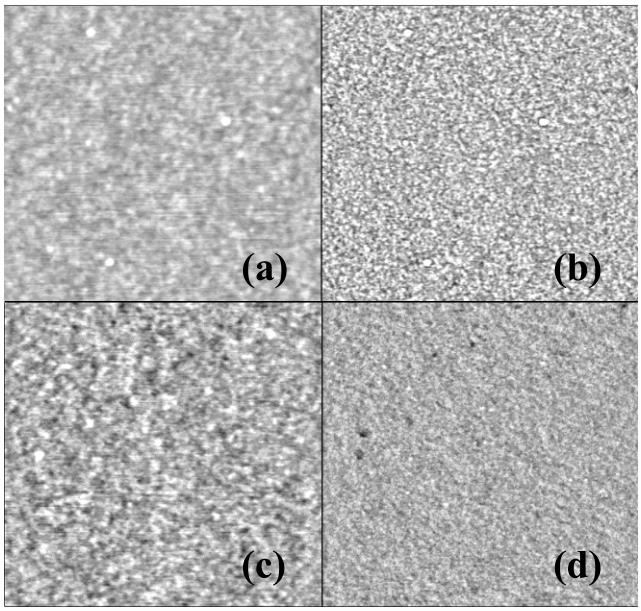

Fig. 4. AFM topographical images (1 × 1 μm) of PBA brush layers fabricated at (a) 15 min, (b) 1 h, (c) 3 h and (d) 18 h grafting time. The vertical scale is 10 nm.

weight tested but decreases to 600 MPa for the layers fabricated from low molar weight PS (Table 2). These values are within a range of values measured for glassy polymers of different molecular weights with AFM probing [52,53]. In contrast, the PBA layer possesses the elastic modulus of 40 MPa, typical for rubbery polymer phases (Table 2). Under identical normal load, the elastic, reversible indentation of the AFM tip is much higher (3–5 times) for the rubbery PBA layer (Fig. 5). Typically, the maximum indentation depth under the normal load of 40 nN was within 3 nm for the rubbery PBA brush layer but stays well below 1 nm for the PS brush layer. The pull-off force normalized to the tip radius R, $\Delta F/R$, could be considered as a measure of adhesive energy required separating the AFM tip and a polymer surface [54,55]. Strong adhesion is observed for the PBA brush layer as expected for rubbery polar polymers (Table 2). The PS brush layer shows consistently smaller adhesion forces as expected for stiffer polymer surfaces with lower surface tension (Table 2).

The elastic modulus of the PS brush layer increases with the molecular weight of the grafted polymers (Table 2, Fig. 6). This trend is continued if additional data points for 'grafted from' brush layer is added [56]. This relationship is

Table 1
Characteristics of PBA polymer brush layer

Grafting time	Film thickness (nm)	RMS roughness (nm)	Grafting amount, Γ (mg/m^2)	Grafting density, Σ (chain/nm^2)	Interchain distance, D (nm)
15 min	1.3	0.20	1.30	0.12	3.25
1 h	2.5	0.19	2.58	0.24	2.31
3 h	3.2	0.19	3.41	0.32	2.00
10 h	3.2	0.18	3.42	0.32	2.00
18 h	3.3	0.17	3.44	0.32	1.99

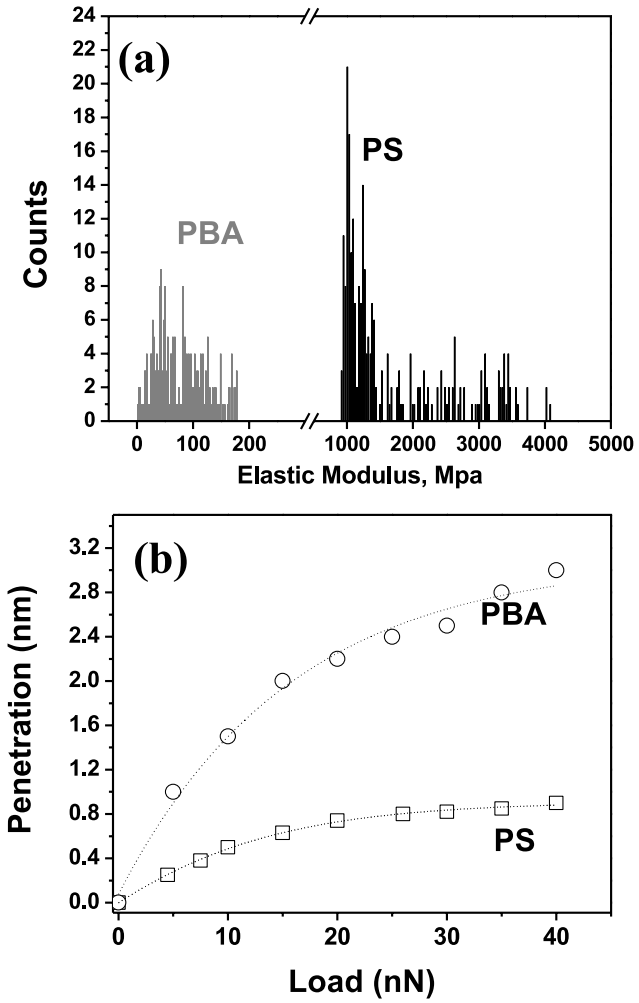

Fig. 5. Histograms of the surface distribution of the micromechanical responses for PBA and PS layers (a) and examples of penetration–load curves for these layers showing very different elastic response on mechanical load (b).

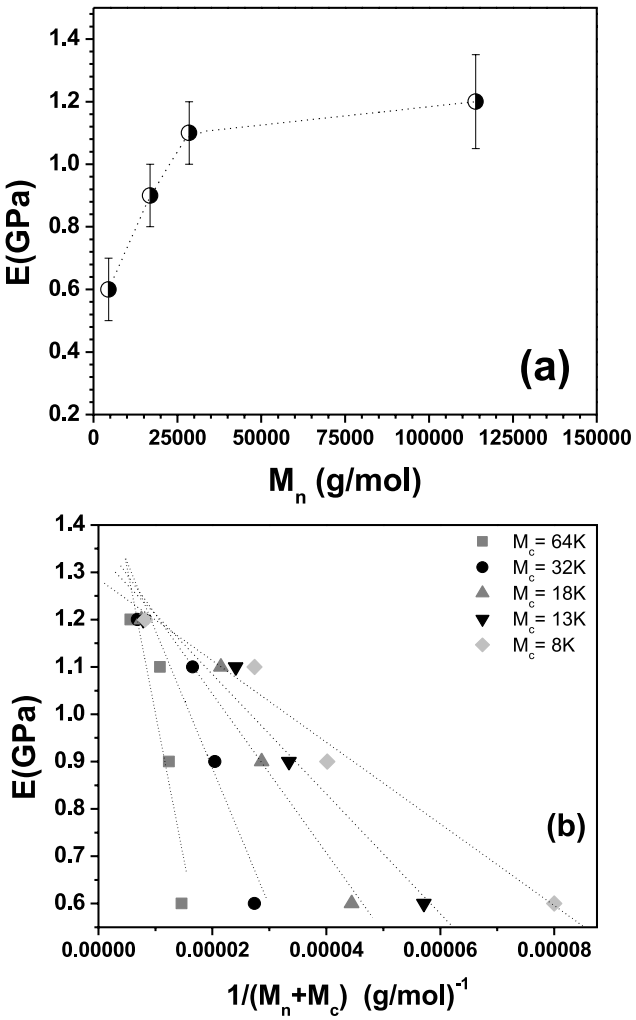

Fig. 6. (a) The elastic modulus versus the molecular weight (M_n) for PS brush layers studied in this work and brush layer from higher molecular weight polymer from Ref. [56] (a). The linear regression fit of the elastic modulus as a function of $1/(M_n + M_c)^{-1}$ with different assumed values of M_c.

reminiscent of the known molecular weight dependence of mechanical properties [57,58]. The increase of mechanical strength is related to the variation of free volume caused by decreasing concentration of end groups of polymer chains and growing constraints imposed by a denser physical network. The formation of a stable entanglement network is expected for molecular weight exceeding a critical segment weight, M_c. As it was established for bulk polymers, strength or elastic modulus, $E(M)$, are a linear function of inverse molecular weight and can be represented as:

$$E(M) = A - B(M + M_c)^{-1} \quad (5)$$

where the parameter A gives an expected value for the polymer with infinite molecular weight and B depends upon chain type [57].

The experimental data of elastic modulus for grafted polymers with different molecular weights analyzed in accordance with Eq. (5) are presented in Fig. 6b. We observed

Table 2
Surface properties of different molecular weight PS and PBA polymer brush layers

Polymers	M_n (g/mol)	Thickness (nm)	Grafting density, Σ (chain/nm^2)	Young's modulus (GPa)	Adhesion (mJ/m^2)
PS	4,500	2.3	0.32	0.6 ± 0.1	19 ± 3
PS	16,900	5.0	0.19	0.9 ± 0.1	20 ± 3
PS	28,500	6.7	0.15	1.1	17 ± 3
PBA	6,500	3.3	0.32	0.03–0.08	37 ± 3

that a good linear fit could be obtained for a whole set of data assuming variation of M_c in a wide range around M_c of 31,000 known for bulk PS [59]. Extrapolation of the linear fit to infinite molecular weight gives an ultimate value of 1.4–1.8 GPa for the reachable elastic modulus of tethered PS chains with high molecular length that is close but a bit lower than usual values of 2.5–3 GPa measured for bulk PS [60]. This difference might indicate that level of short range ordering in grafted polymer chains is somewhat lower than in the bulk state and additional disturbance due to the presence of spatial constraints leads to weaker compression resistance of ultrathin grafted polymer layers. Three PS brush layers studied here represent very different cases of chains with few entanglements for $M \ll M_c$ as well as chains with stable entanglement network for polymer brushes with $M \sim M_c$. This transition between these two states shows itself in dramatic reduction of the compliance reflected in twofold increase in the elastic modulus for grafted layers with $M \sim M_c$. These dramatic changes of the elastic properties of polymer brushes are observed in the range of molecular weights close to the critical segment length of amorphous PS. It could be expected that actual M_c value for tethered polymer chains is higher than for unconstrained random coils. However, it seems that spatial constrains imposed by tethered chain ends only modestly influences the formation of chain entanglements in thin brush layer. Unfortunately, a limited number of molecular weights prevents us of making a firm conclusion on this issue.

Acknowledgements

This research is supported by the National Science Foundation, CMS-0099868 Grant and Grant M01-C03 from Department of Commerce through National Textile Center. The authors thank H. Shulha for useful discussions and assistance.

References

[1] Halperin A, Tirrell M, Lodge TP. Adv Polym Sci 1992;100:33.
[2] Milner ST. Science 1991;251:905.
[3] Klein J. Ann Rev Mater Sci 1996;26:581.
[4] Hsu SM. Tribol Lett 1997;3:1.
[5] Gellman AJ. Curr Opin Colloid Interface Sci 1998;3:368.
[6] Bhushan B, Zhao Z. J Info Storage Proc Syst 1999;1:1.
[7] Berman A, Steinberg S, Campbell S, Ulman A, Israelachvili JN. Tribol Lett 1998;4:43.
[8] Ruths M, Johannsmann D, Rühe J, Knoll W. Macromolecules 2000;33:3860.
[9] Butt HJ, Kappl M, Mueller H, Raiteri R. Langmuir 1999;15:2559.
[10] Schorr P, Kwan TCB, Kilbey SM, Shaqfeh ESG, Tirrell M. Macromolecules 2003;36:389.
[11] Dolan AK, Edwards SF. Proc R Soc London A 1974;337:509.
[12] Alexander S. J Phys (Paris) 1977;38:983.
[13] de Gennes PG. Macromolecules 1980;13:1069.
[14] de Gennes PG. Adv Colloid Interface Sci 1987;27:189.
[15] Karim A, Tsukruk VV, Douglas JF, Satija SK, Fetters LJ, Reneker DH, Foster MD. J Phys II France 1995;5:1441.
[16] Auroy P, Auvray L, Leger L. Macromolecules 1991;24:5158.
[17] Norton LJ, Smiglova V, Pralle MU, Hubenko A, Dai KH, Kramer EJ, Hahn S, Begrlund C, DeKoven B. Macromolecules 1995;28:1999.
[18] Dijt JC, Cohen Stuart MA, Fleer GJ. Macromolecules 1994;27:3207.
[19] Jones RAL, Lehnert RJ, Schonerr H, Vancso J. Polymer 1999;40:525.
[20] Luzinov I, Julthongpiput D, Malz H, Pionteck J, Tsukruk VV. Macromolecules 2000;33:1043.
[21] Tsukruk VV, Luzinov I, Julthongpiput D. Langmuir 1999;15:3029.
[22] Luzinov I, Julthongpiput D, Liebmann-Vinson A, Cregger T, Foster MD, Tsukruk VV. Langmuir 2000;16:504.
[23] Motschmann H, Stamm M, Toprakcioglu CH. Macromolecules 1991;24:3681.
[24] Xie R, Karim A, Douglas JF, Han CC, Weiss RA. Phys Rev Lett 1998;81:1251.
[25] Liu Y, Rafailovich MH, Sokolov J, Schwarz SA, Zhong X, Eisenberg A, Kramer EJ, Sauer BB, Satija S. Phys Rev Lett 1994;73:440.
[26] Koneripalli N, Singh N, Levicky R, Bates FC, Gallagher PD, Satija SK. Macromolecules 1995;28:2897.
[27] Handbook of fine chemicals and laboratory equipment, Aldrich®, 2003.
[28] Tsukruk VV. Rubber Chem Technol 1997;70(3):430.
[29] Tsukruk VV, Reneker DH. Polymer 1995;36:1791.
[30] Luzinov I, Julthongpiput D, Gorbunov V, Tsukruk VV. Tribol Int 2001;35:327.
[31] Tsukruk VV, Wahl K, editors. Microstructure and microtribology of polymer surfaces. ACS Symposium Series, vol. 741.; 2000.
[32] Cleveland J, Manne S, Bocek D, Hansma PK. Rev Sci Instrum 1993;64:403.
[33] Hazel J, Tsukruk VV. J Tribol 1998;120:814.
[34] Tsukruk VV, Gorbunov V. Microsc Today 2001;01-1:8.
[35] Tsukruk VV, Huang Z, Chizhik SA, Gorbunov VV. J Mater Sci 1998;33:4905.
[36] Tsukruk VV, Gorbunov VV, Huang Z, Chizhik SA. Polym Int 2000;49:441.
[37] Makushkin AP. Friction Wear 1990;11:423.
[38] Giannakopoulos AE, Suresh S. Int J Solids Struct 1997;34:2393.
[39] Tsukruk VV, Gorbunov VV. Probe Microsc 2002;3–4:241.
[40] Henn G, Bucknall DG, Stamm M, Vanhoorne P, Jerome R. Macromolecules 1996;29:4305.
[41] Luzinov I, Julthongpiput D, Tsukruk VV. Macromolecules 2000;33:7629.
[42] Quali L, Francois A, Pefferkorn E. J Colloid Interface Sci 1999.
[43] Yeung C, Balaz AC, Jasnow D. Macromolecules 1993;26:1914.
[44] Kelley TW, Schorr PA, Johnson KD, Tirrell M, Frisbie CD. Macromolecules 1998;31:4297.
[45] Tang H, Szleifer I. Europhys Lett 1994;28:19.
[46] Auroy P, Auvray L, Leger L. Phys Rev Lett 1991;66:719.
[47] Siqueira DF, Köhler K, Stamm M. Langmuir 1995;11:3092.
[48] Lai PY, Binder K. J Chem Phys 1992;97:586.
[49] Ligoure C, Leiber L. J Phys (Paris) 1990;51:1313.
[50] Hadziioannou G, Patel S, Granick S, Tirell M. J Am Chem Soc 1986;108:2869.
[51] Taunton H, Toprakcioglu C, Fetters L, Klein J. Nature (London) 1988;332:712.
[52] Chizhik SA, Huang Z, Gorbunov VV, Myshkin NK, Tsukruk VV. Langmuir 1998;14:2606.
[53] Tsukruk VV, Sidorenko A, Yang H. Polymer 2002;43:1695.
[54] Noy IA, Vezenov DV, Lieber CM. Annu Rev Mater Sci 1997;27:381.
[55] Noy A, Daniel Frisbie C, Rozsnyai LF, Wrighton MS, Lieber CM. J Am Chem Soc 1995;117:7943.
[56] Lemieux M, Minko S, Usov D, Stamm M, Tsukruk VV, accepted for publication.
[57] Fox TG, Flory PJ. J Appl Phys 1950;21:581.
[58] Fox TG, Flory. J Polym Sci 1954;14:315.
[59] Fried JR, editor. Polymer science and technology. Englewood Cliffs: PTR Prentice Hall; 1995.
[60] Sperling LH, editor. Introduction to physical polymer science. New York: Wiley-Interscience; 1992.